Le PLUG-IN
NX de WAVES

NX 9-91-63-8 Build E 122366 (Cocoa)

Bernard Lagnel   Novembre 2017

http://www.lesonbinaural.fr

WAVES NX : HRTF pour une source <u>Mono</u> à 30°

INPUT

OUTPUT

ENTRÉE MONO

SORTIE STÉRÉO BINAURALISÉE

A: Initial Preset*

Load   Save   ?

A→B

HEAD TRACKING   OFF

TRACKING DEVICE

Cam>ora FaceTi... (int>@gr>@e ⌄

RESTART   SWEET SPOT

TRACKING RATE   XYZ LOCK

0

G   D

HEAD MODELING   ?

BERNARD   ⌄

CIRCUMFERENCE   UNITS

58.0   CM

INTER-AURAL ARC   INCH

28.0

ROOM AMBIENCE

50

0   100

AMOUNT

SPEAKER POSITION

30.0

0°

+/- 180°

ROTATE

0

GAIN

DIFFRACTION DE LA TÊTE HUMAINE :

Modèle = Sphère de 18 cm de Ø

90° 0 dB
105°   75°
120°   60°
135°   45°
-5 dB
150°   30°
Données
-10 dB   Schoeps
165°   KFM 360   15°
-15 dB
180°   -20 dB   r = 9 cm   0°
195°   345°
210°   330°
225°   315°
240°   300°
255°   285°
270°

Légende :
- 500 Hz
- 1 KHz
- 2 KHz
- 4 KHz
- 8 KHz
- 16 KHz

Kr = 0,1   Kr = 1   Kr = 10   Kr = 100

+5 dB   θ=0°
θ=90°
0 dB
θ=105°
-5 dB
-10 dB   θ=150°   θ=120°
θ=165°   θ=135°
-15 dB   θ=180°

60 Hz   170 Hz   600 Hz   1,7 KHz   6 KHz   17 KHz   60 KHz

$$Kr = 2\pi r/\lambda$$

onde incidente
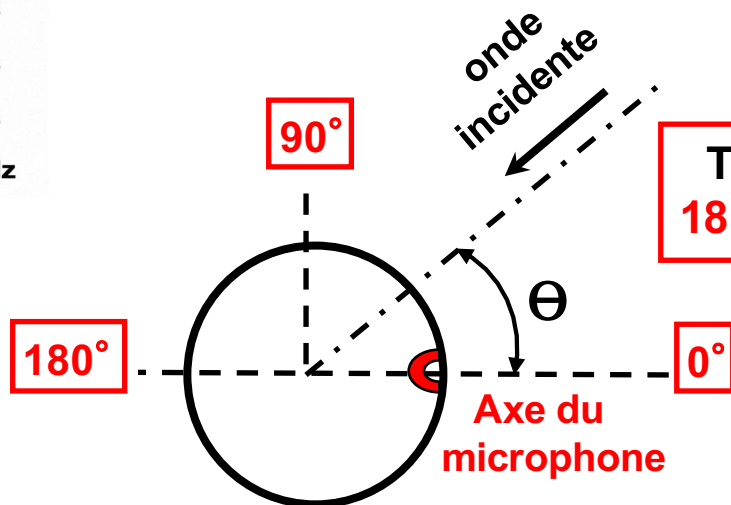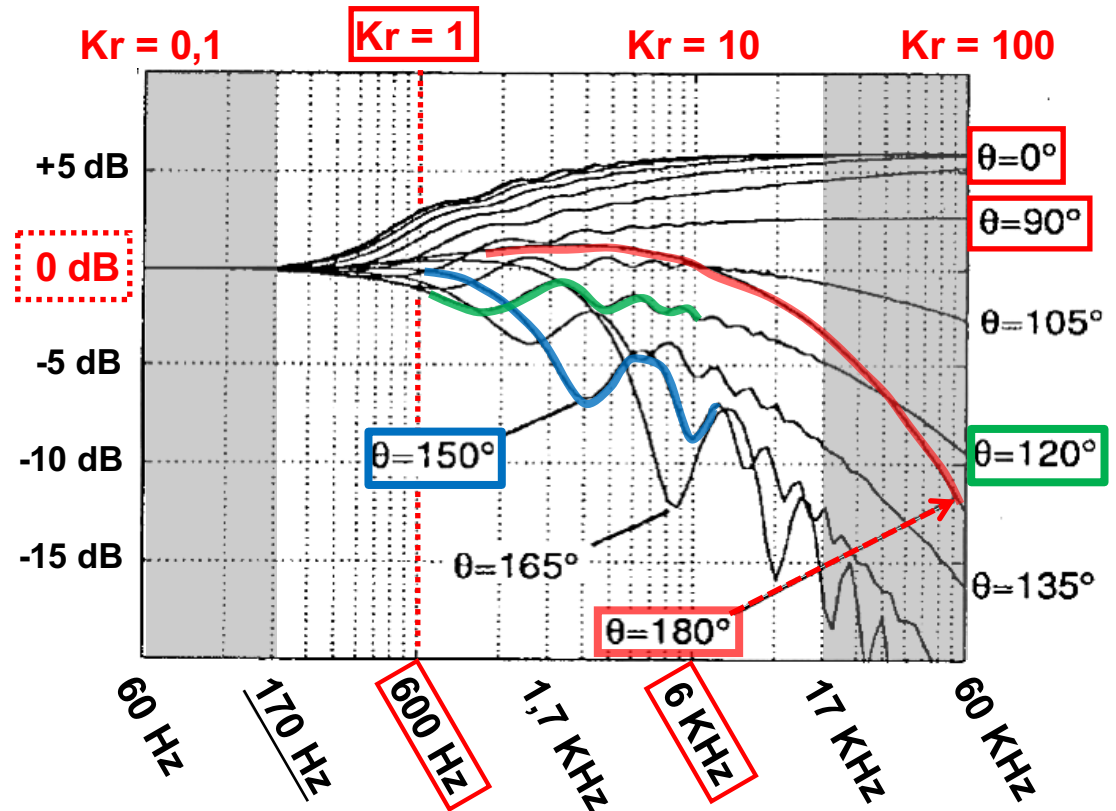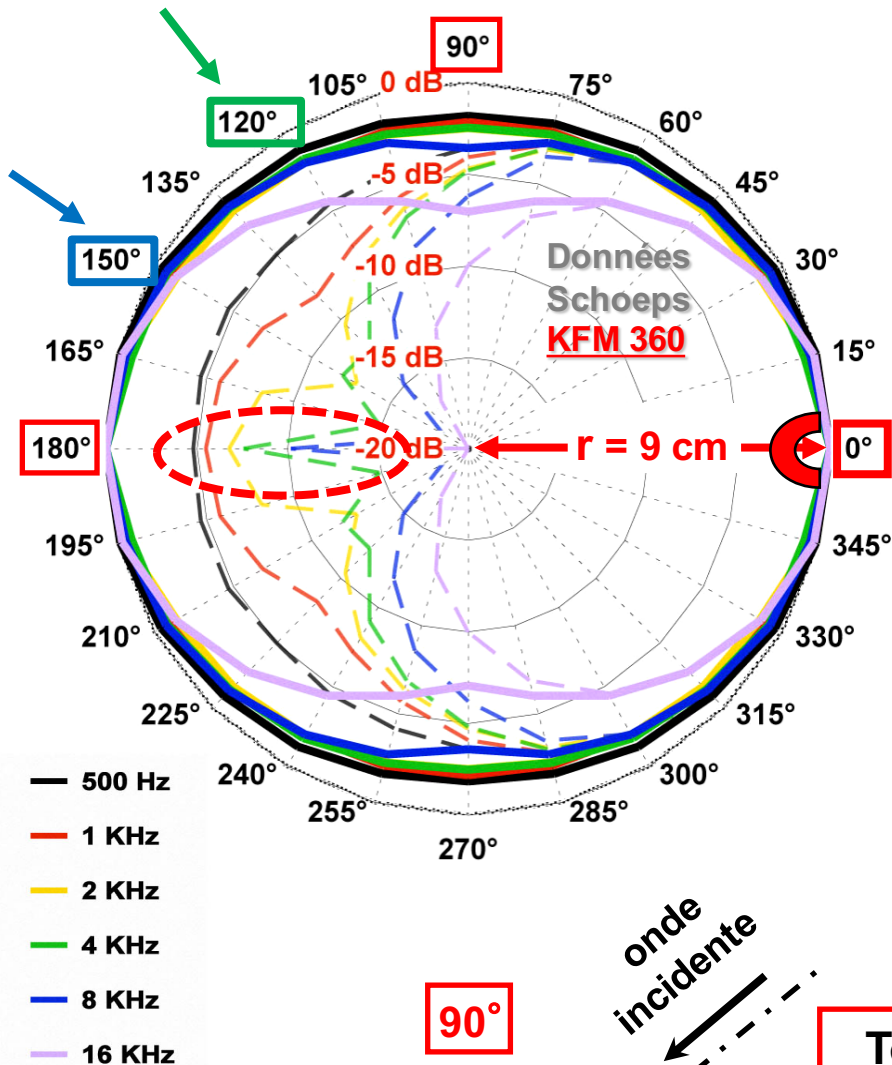
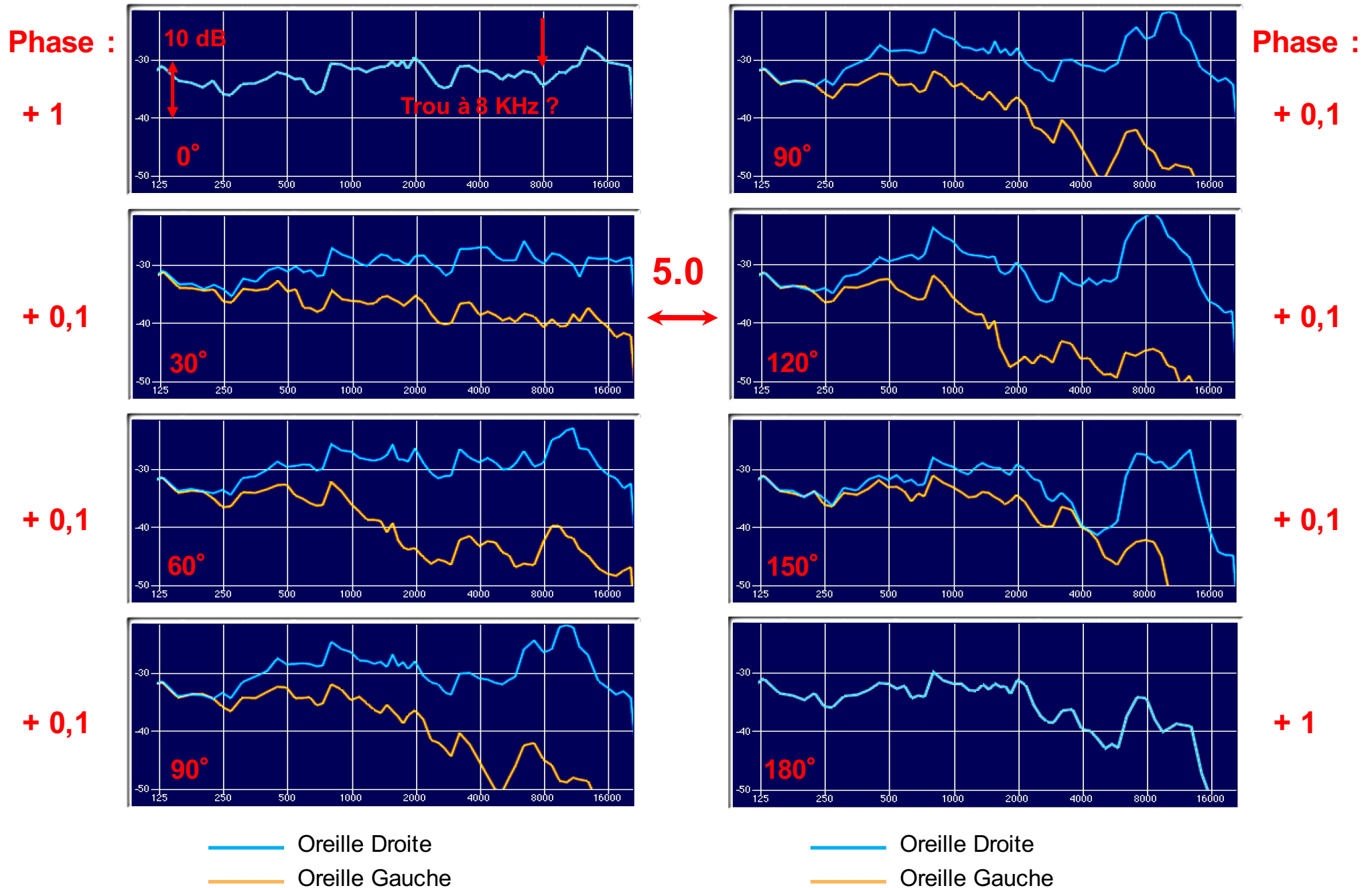Tour de tête pour
18 cm de Ø = 56,5 cm

90°
Θ
180°   0°
Axe du
microphone

Pour Kr = 1 :

$$F = C/(2\pi r)$$

$$F \approx 600 \text{ Hz}$$

(C = Célérité du son)

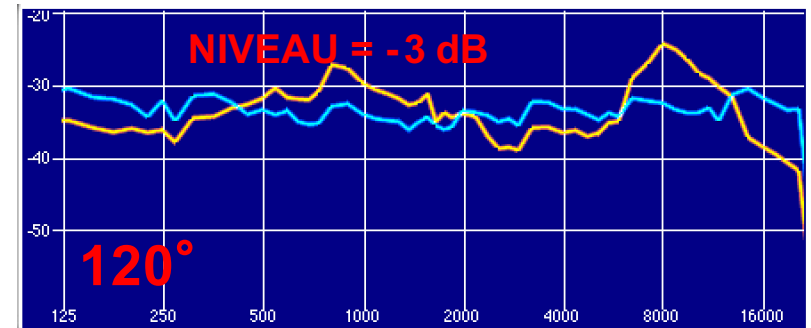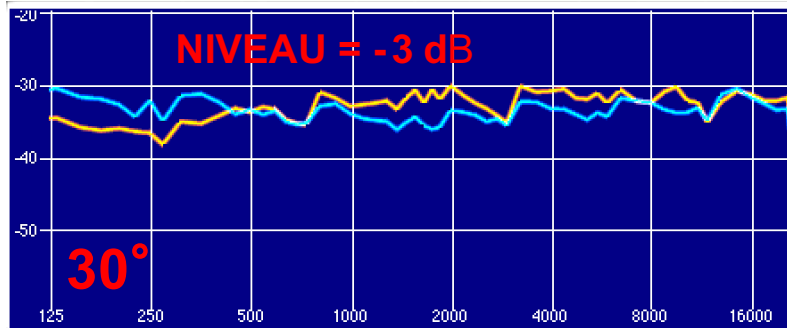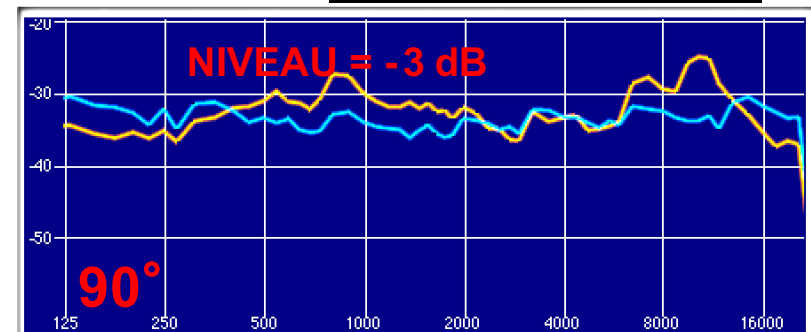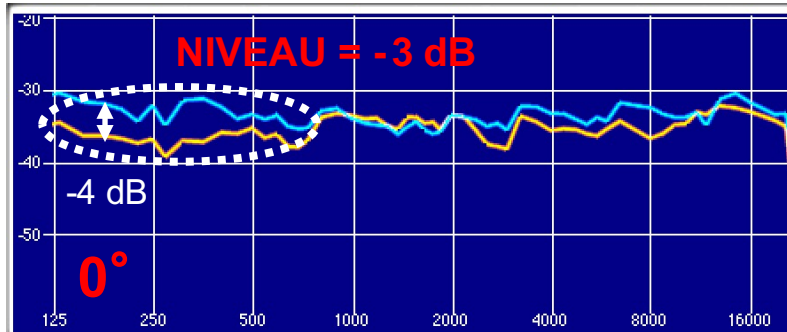# WAVES NX : HRTF pour une source <u>Mono</u> se déplaçant vers la Droite
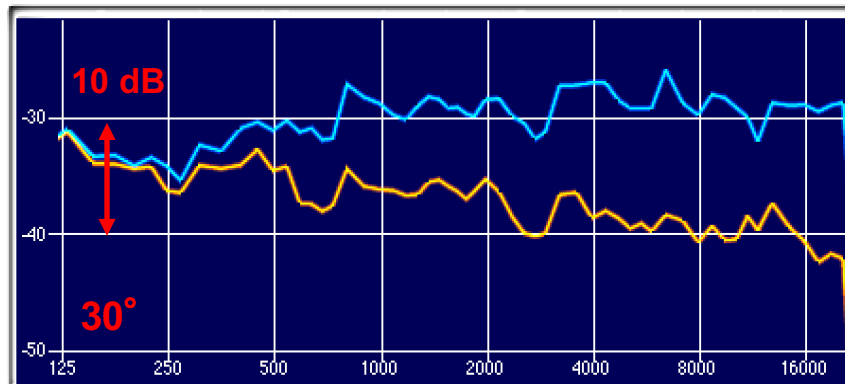
HRTF et Bruit Rose : Nx de WAVES

WAVES NX : HRTF pour une source <u>Mono</u> se déplaçant vers la Droite

WAVES NX : HRTF pour une source **Stéréo** à 30° et à 120°

NX 9-91-63-8 Build E 122366 (Cocoa)

HP

ENTRÉE STÉRÉO

SORTIE STÉRÉO BINAURALISÉE

Casque en 3D

Chemins croisés : Modèle de Woodworth

Modèle de Woodworth (1962)

Circonférence de ma tête **Cir**	Angle de la source
58 cm	30 °

ΔT = différence de marche du couple		ΔT en échantillons pour du 48 KHz
9,4 cm	0,3 ms	13

+0,3

-0.5   0   +0.5

-1   +1

CORRELATION
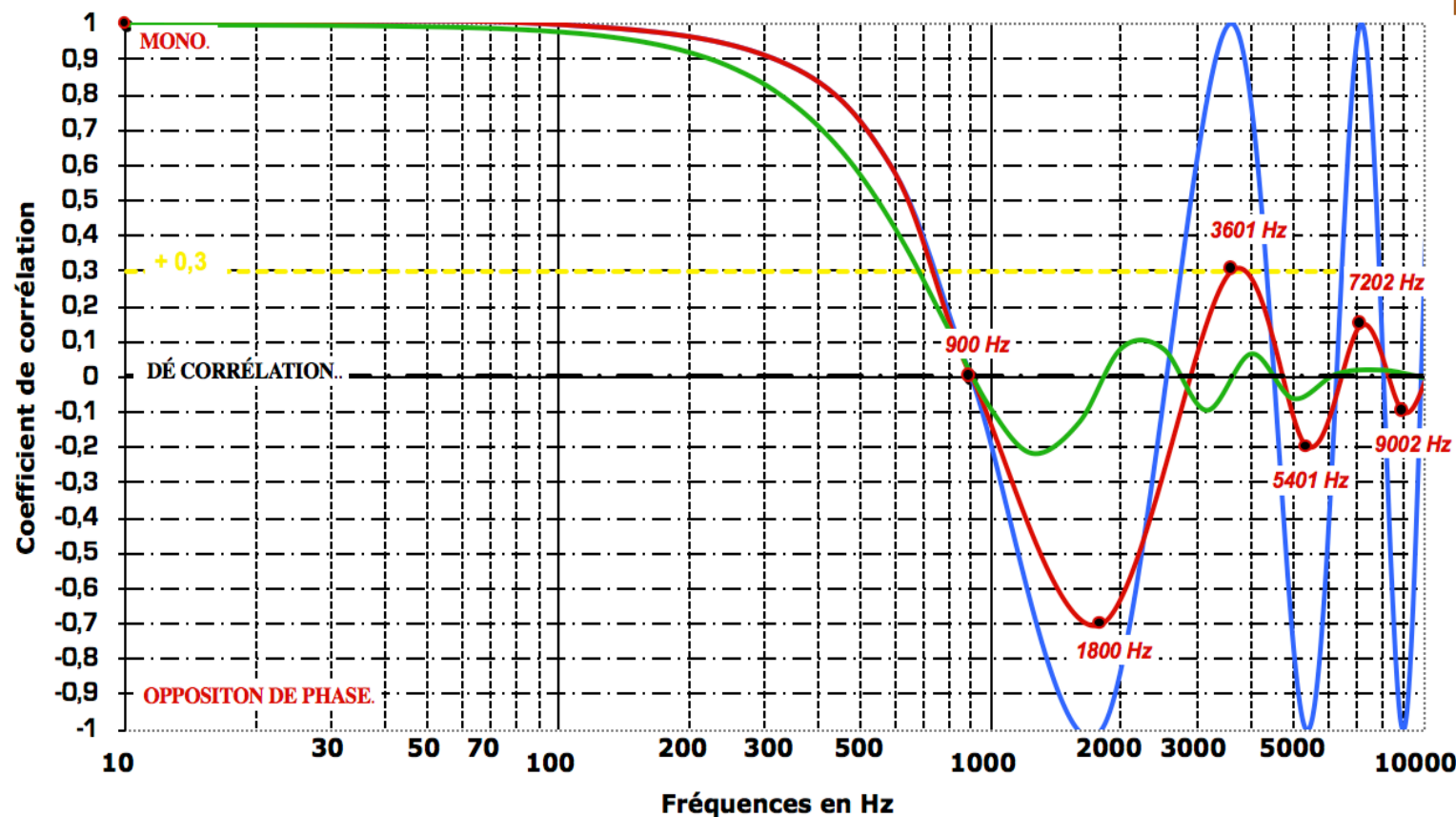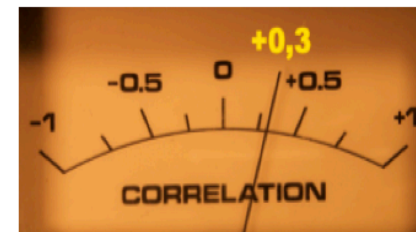
- - - PHASEMÈTRE à +0,3 RÉPARTITION HOMOGÈNE DE L'IMAGE STÉRÉO

—— FILTRE EN PEIGNE THÉORIQUE SUR TOUT LE SPECTRE AUDIBLE DÛ A LA SOMMATION DES 2 CANAUX

—— CAPTATION DE SOURCES SONORES COMPLEXES EN CHAMP PROCHE

—— CAPTAION DANS LE CHAMP DIFFUS

2009 Bernard Lagnel

Coefficient de corrélation (axe vertical, de 1 à -1)

MONO.

+ 0,3

DÉ CORRÉLATION.

OPPOSITON DE PHASE.

900 Hz, 1800 Hz, 3601 Hz, 5401 Hz, 7202 Hz, 9002 Hz

Fréquences en Hz

Filtrage en peigne pour une source Stéréo à 30°

$$\Delta T = (\ \mathbf{Cir}\ /\ (2\ \pi \times 340)\ ) \times (\ (\ \pi\ /\ 6\ ) + \sin 30°\ )$$

Pour ma tête à 30° : ΔT = 0,28 ms

TRIGONOMÉTRIE
Correspondance degré-radian

Degrés	0°	30°	45°	60°	90°	120°	135°	150°	180°	360°
Radians	0	$\frac{\pi}{6}$	$\frac{\pi}{4}$	$\frac{\pi}{3}$	$\frac{\pi}{2}$	$\frac{2\pi}{3}$	$\frac{3\pi}{4}$	$\frac{5\pi}{6}$	π	2π

WAVES NX : HRTF pour une source <u>Stéréo</u>

Input Bruit Rose
(corrélation entre G et D = +0,5) :
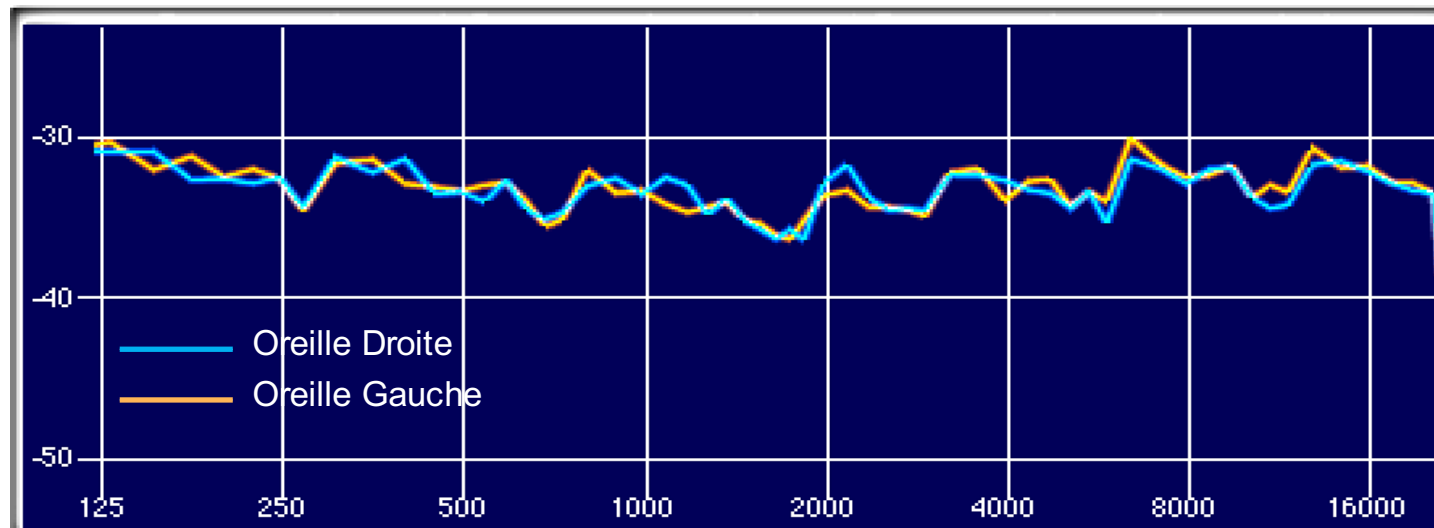
Output Waves NX en Binaural
(corrélation entre G et D = +0,5 à +0,6) :

WAVES NX : HRTF pour une source Stéréo

WAVES NX : HRTF pour une source **Stéréo**

NX 9-91-63-8 Build E 122366 (Cocoa)

Pour le 5.0

Pour le 4.0

30° 120° 45° 135°
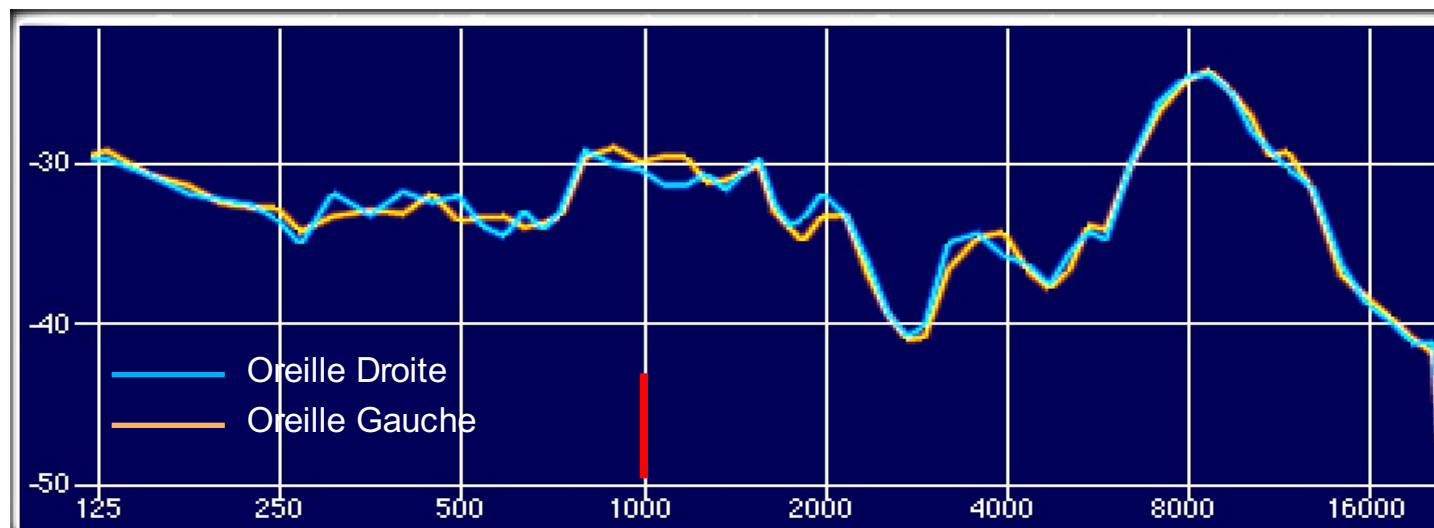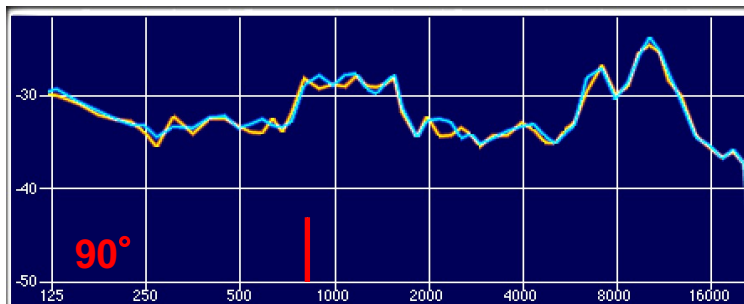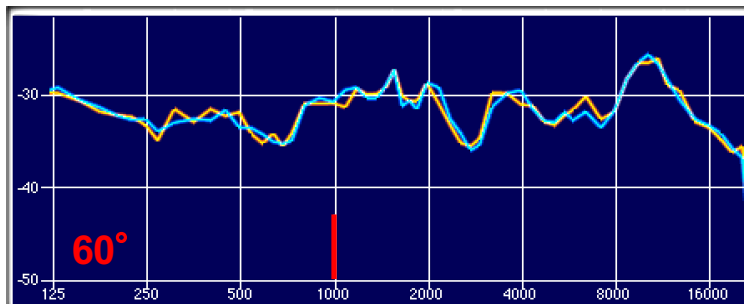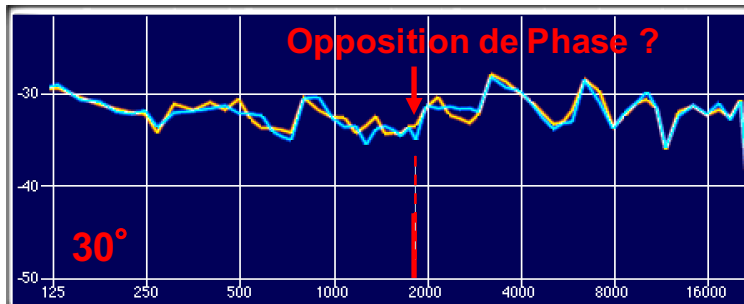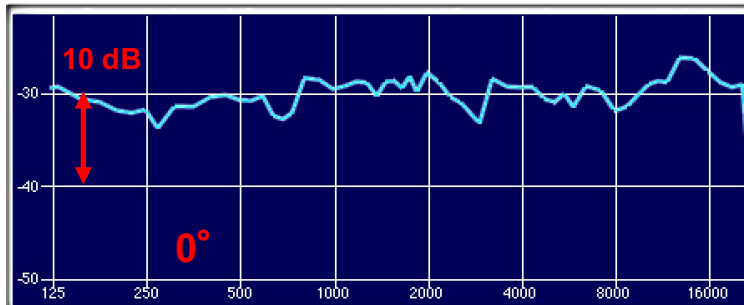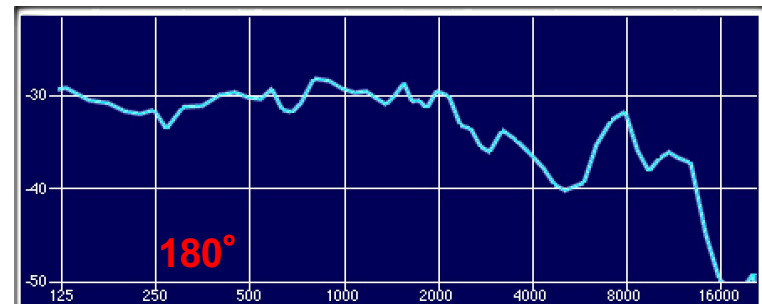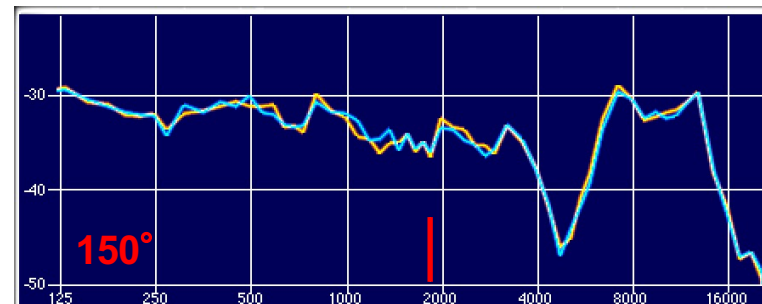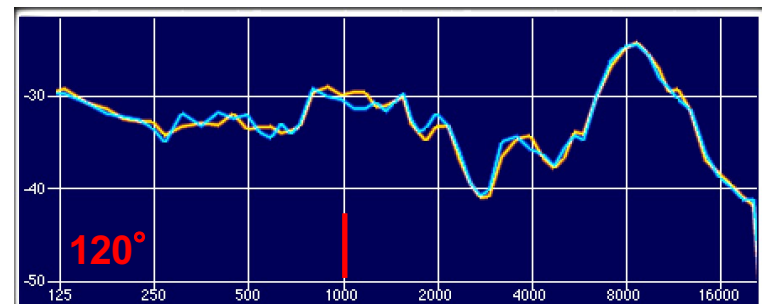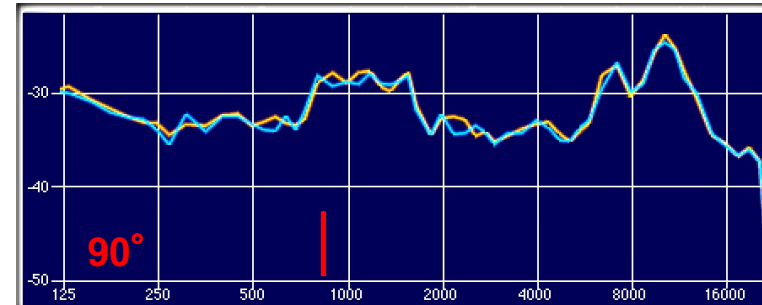
Oreille Droite
Oreille Gauche

WAVES NX : HRTF pour une source <u>Stéréo</u> à 30° et à 120°

30°

120°
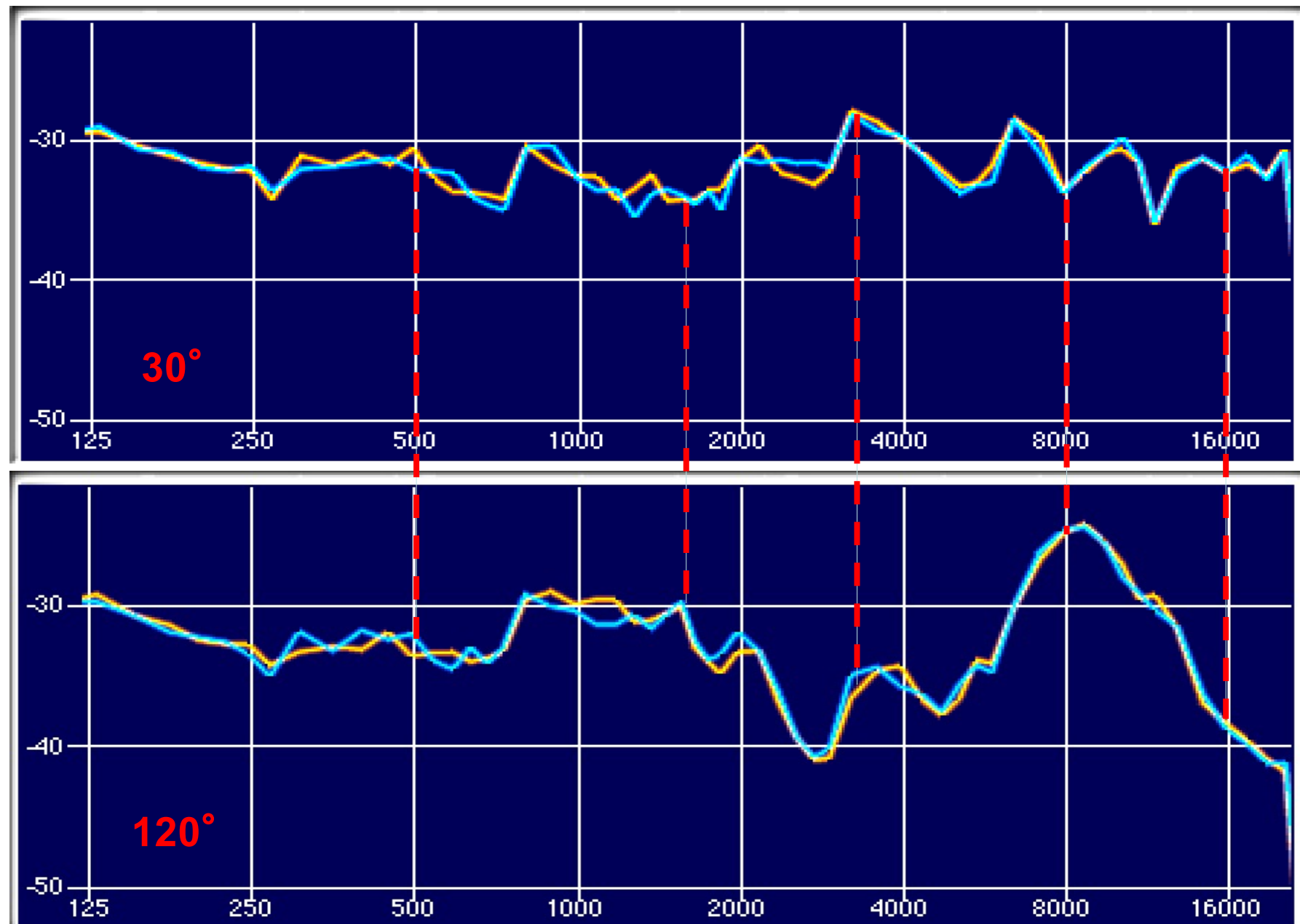
Corrections à apporter pour *"binauraliser en partie"* du multicanal :

Pour le 5.0

- NX à 30°
- NX à 120°

Pour le 4.0

- NX à 45°
- NX à 135°

NX 9-91-63-8 Build E 122366 (Cocoa)
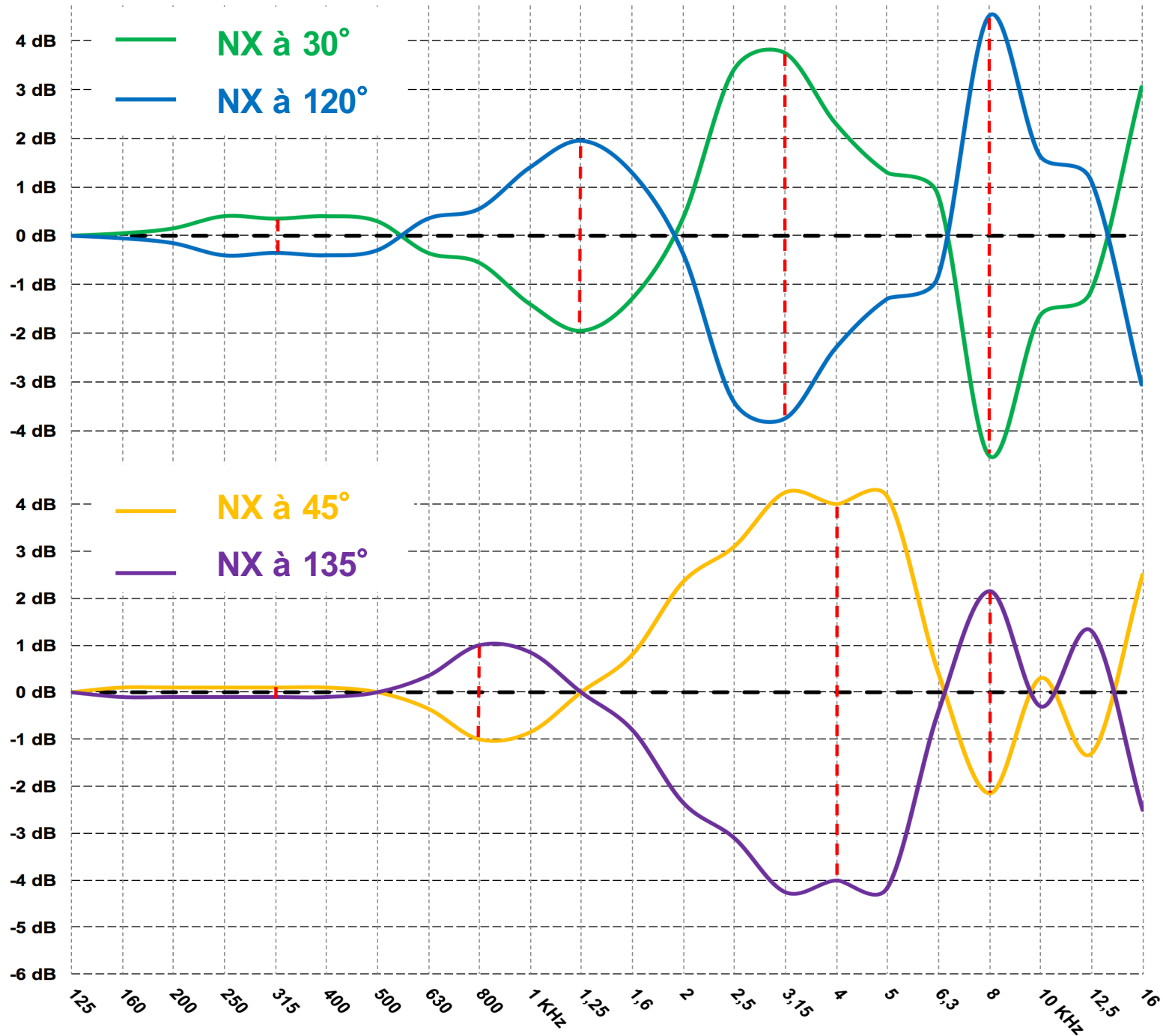
Fréquence relative des jugements en % : Devant 0° et Derrière 180°
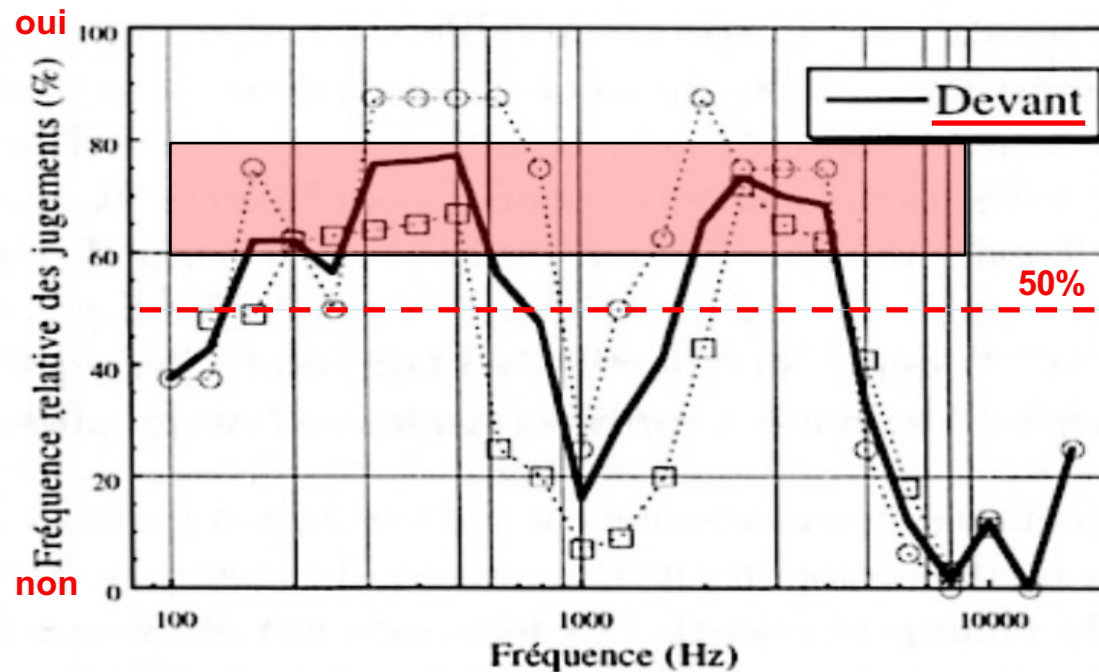
Direction apparente de sons présentés dans le plan médian. Les points de mesure sont empruntés à Blauert 1969 pour les symboles carrés et à Chateau 1995 pour les symboles ronds.
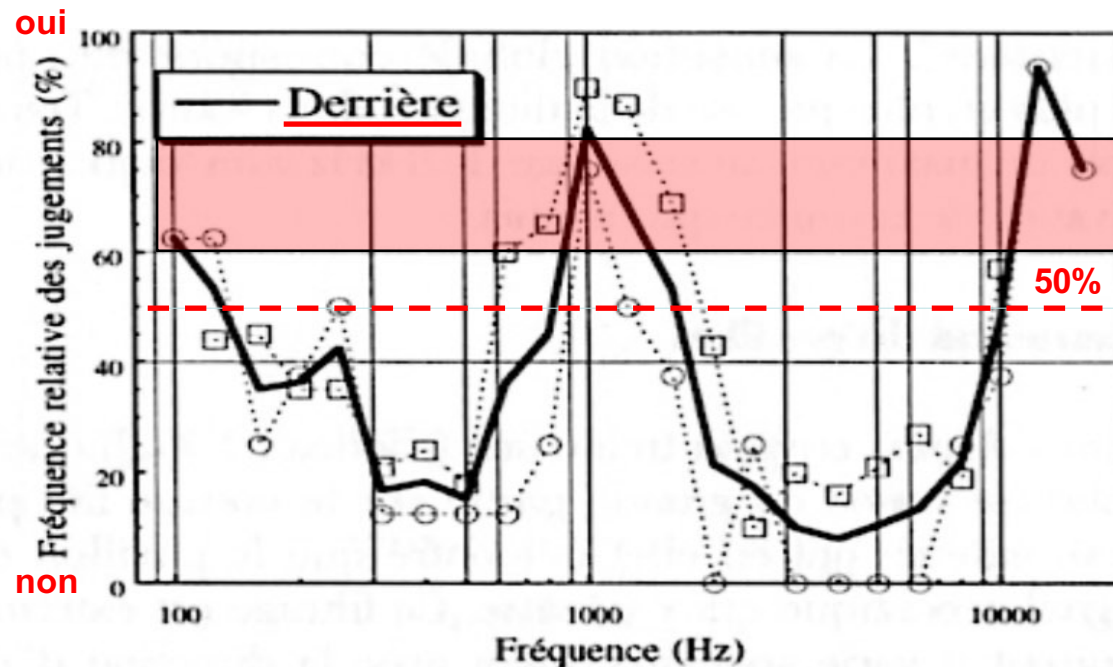
Domaine **cognitif sensoriel** dans un environnement **3D**
Les **HRTF** *de* **Robinson & Whittle** *1960 :*

AZIMUT

ÉLÉVATION

- 4000 Hz
- 8000 Hz

- 8000 Hz
- 4000 Hz
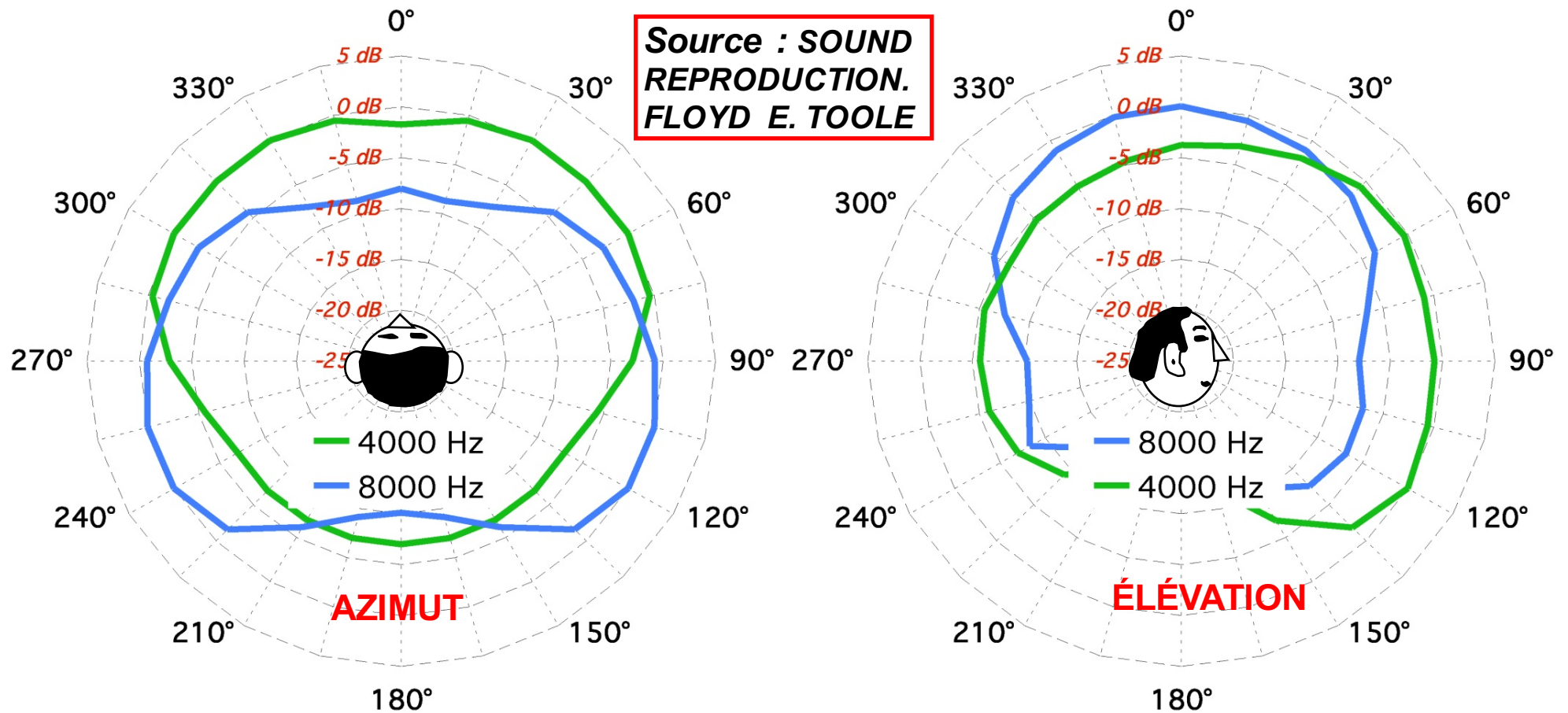
Directivité " marquée " de 2 fréquences : 4 kHz et 8 kHz

- le **4 kHz** = (présence / absence) ou la perception des distances
- le **8 kHz** = (brillance / mat) et l'Espace sonore en **3D**

Domaine **cognitif sensoriel** dans un environnement **3D**

Les *HRTF* de **Robinson & Whittle** *1960 :*
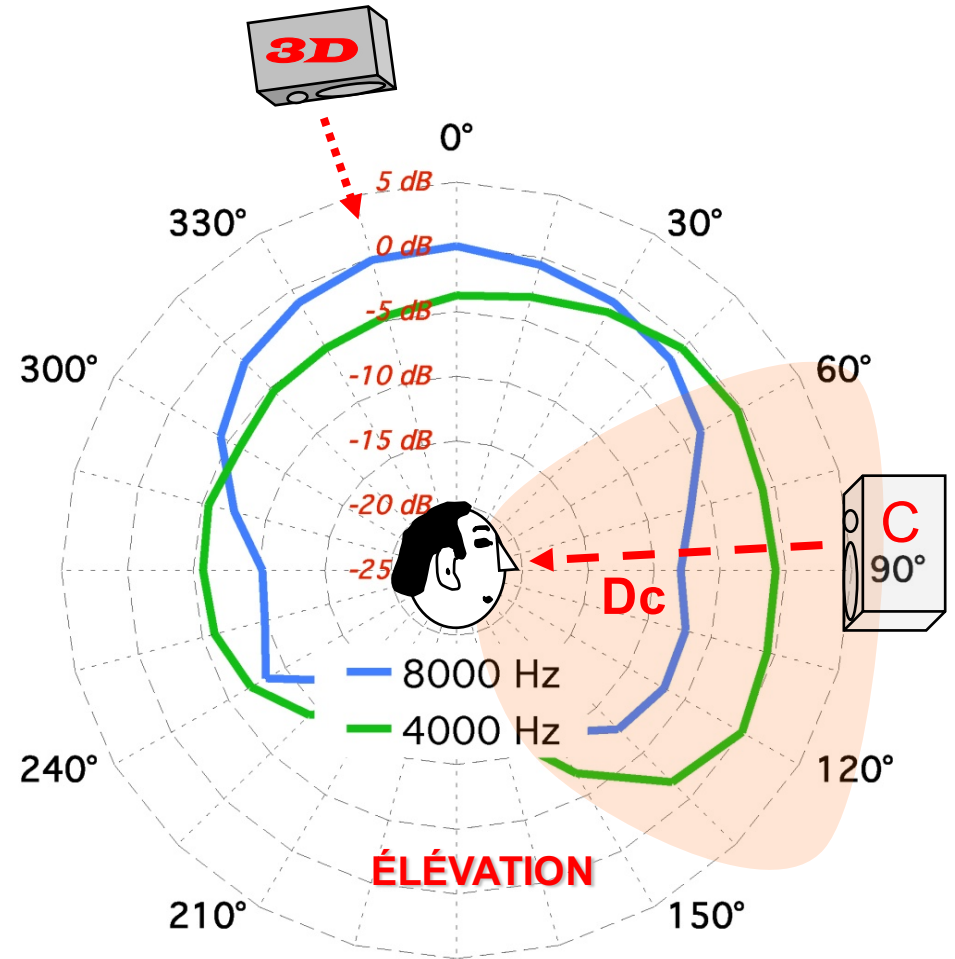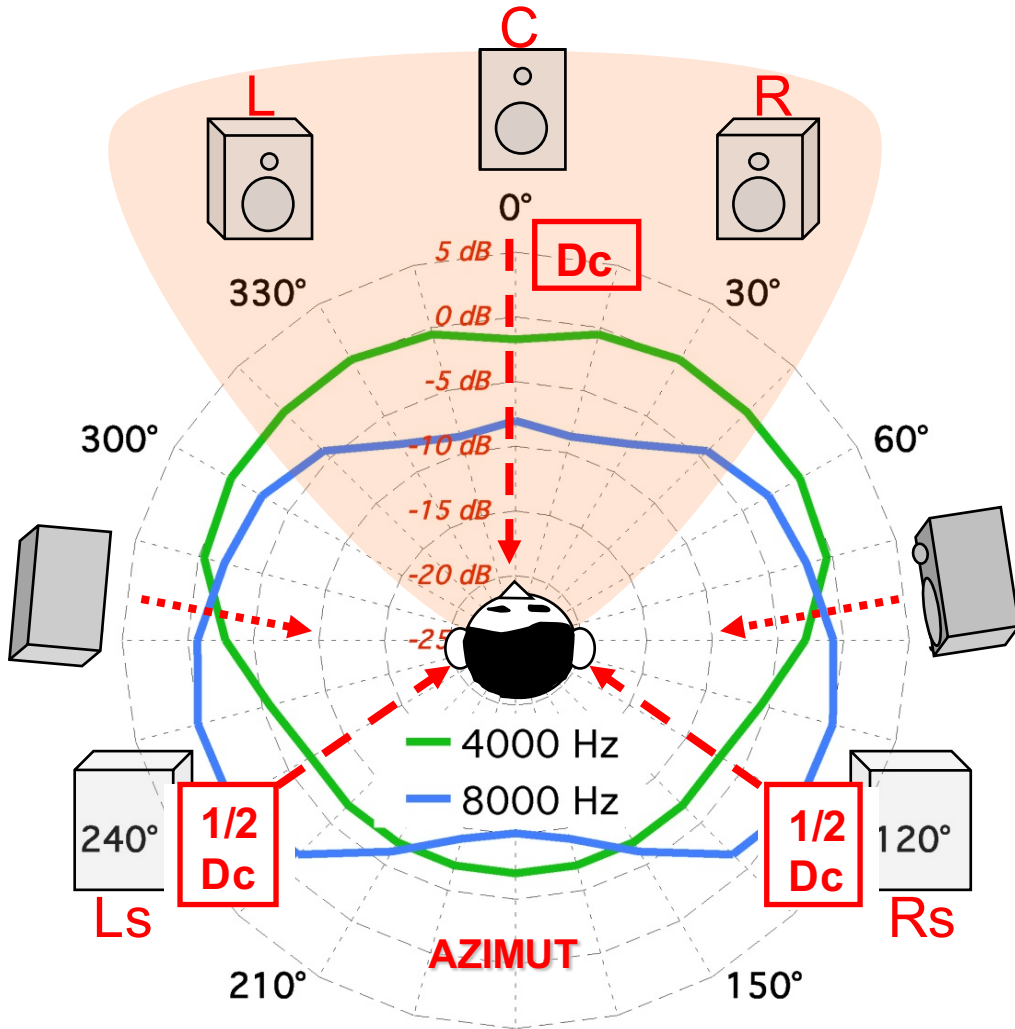
Localisation instable d'une source fantôme entre **R** et **Rs** ⟹ **7.0**

Dc est mal perçue à l'arrière (Ls Rs) ⟹ délai pour **conformité** ITU.

COMPARAISON ENTRE L'_AUDITION_ ET LA _VISION_ :

⇔ 4 KHz

Rétine Centrale :

- Présence de _cônes_
- Faible sensibilité
- Forte acuité
- Traite les informations relatives à la _forme_ et à la couleur
- Rôle : _Reconnaissance_ de l'information…

⇔ 8 KHz

Rétine Périphérique :

- Présence de _bâtonnets_
- Forte sensibilité
- Faible pouvoir de discrimination
- Traite les informations relatives au _mouvement_
- Rôle : _Détection_ de l'information et du ⚠️

wikipedia.org/Rétine

L'enregistrement binaural :

Diffusion et Réflexion pour un **objet de dimension ≥ 1/2 $\times \lambda$**

PAVILLON pour l'espace *frontal*.

4 cm ≈ 1/2 $\times \lambda$ (à 4 kHz)

2 cm ≈ 1/2 $\times \lambda$ (à 8 kHz)

TRAGUS pour l'espace *dorsal*.

BL 2012

DPA 4060 + DUA0560

MASQUE LE TRAGUS

ADPHOX BME-200

ROLAND CS-10EM

Merci de votre attention

Site : **http://www.lesonbinaural.fr**

Mail : **b.lagnel@gmail.com**

PHOTOS Bernard Lagnel

Testing, correcting, and extending the Woodworth model for interaural time difference

Neil L. Aaronson
Natural Science and Mathematics, Richard Stockton College of New Jersey, 101 Vera King Farris Drive, Galloway, New Jersey 08205

William M. Hartmann[a]
Department of Physics and Astronomy, Michigan State University, 567 Wilson Road, East Lansing, Michigan 48824

The Woodworth model and formula for interaural time difference is frequently used as a standard in physiological and psychoacoustical studies of binaural hearing for humans and other animals. It is a frequency-independent, ray-tracing model of a rigid spherical head that is expected to agree with the high-frequency limit of an exact diffraction model. The predictions by the Woodworth model for antipodal ears and for incident plane waves are here compared with the predictions of the exact model as a function of frequency to quantify the discrepancy when the frequency is not high. In a second calculation, the Woodworth model is extended to arbitrary ear angles, both for plane-wave incidence and for finite point-source distance. The extended Woodworth model leads to different formulas in six different regions defined by ear angle and source distance. It is noted that the characteristic cusp in Woodworth's well-known function comes from ignoring the longer of the two paths around the head in circumstances when the longer path is actually important. This error can be readily corrected. © *2014 Acoustical Society of America.* [http://dx.doi.org/10.1121/1.4861243]

I. INTRODUCTION

The Woodworth model and formula[1] compute the interaural time difference (ITD) for a human listener or other animal assuming that the head is a rigid sphere and that the ears are antipodal points. The model appeared in the textbook by Woodworth (1938) without derivation or qualifications and is based on ray tracing with simple geometry. The formula was found to be in excellent agreement with the interaural delay for clicks measured on human listeners by Feddersen *et al.* (1957), and it has been used often in binaural acoustics (e.g., Carlile, 1996; Schnupp *et al.*, 2003) and binaural synthesis (e.g., Brown and Duda, 1998; Nam *et al.*, 2008).

The Woodworth model is physically valid when the wavelength of the sound is much smaller than the radius of the head. For a head of radius 87.5 mm in room-temperature air, this corresponds to frequencies above about 4 kHz. In this article, we show, by means of a straightforward but extensive numerical calculation, that the model and its creeping wave solution approach the high-frequency limit of the exact diffraction equation developed by Rayleigh (1896) and made more accessible by Rschevkin (1963), Kuhn (1977), and by Duda and Martens (1998). The numerical calculation establishes the limits of validity of the formula as the frequency of the sound departs from infinity and quantifies the error in Woodworth's approximation. The error can be considerable when the assumptions of the model are not respected. This article also extends the Woodworth model so that it applies when sources are a finite distance away from

the head and when the ears are not antipodal. The extended model can be useful when the spectrum of the signal is not known exactly so that the exact diffraction model is not applicable. Elements of this extension have been given in previous literature, as will be noted in the following text, but the extension given here is complete. The extensions are useful when the ray-tracing assumptions of the original model are valid, but the geometry differs from the original.

II. WOODWORTH MODEL AS A LIMIT

The Woodworth model assumes a rigid, spherical head and a source of sound at some azimuth angle with respect to the forward direction so that the source is closer to one ear than to the other. The ITD is given by the extra path length to the far ear divided by the speed of sound. In turn, the path lengths are computed by ray-tracing geometry. The path length from a source to an unoccluded ear is the straight-line distance between the source and the ear. The path length to an occluded ear is given by the straight-line path of a tangent to the sphere plus the arc length from the point of tangency to the ear. Thus it is assumed that the wave creeps around the surface of the head to an occluded ear. Only the shortest arc length is included in the calculation for an occluded ear. The wave that creeps around the far side of the head is neglected.

A. Woodworth formula, antipodal ears

Woodworth's model for the ITD assumed that the arriving sound is a plane wave (infinite source distance) and that the ears are 90° back from the forward direction (ear angle of 90°). With those assumptions, there are two formulas for the ITD for a source on the right side of the head,

[a]Author to whom correspondence should be addressed. Electronic mail: hartmann@pa.msu.edu

$$\text{ITD} = (a/c)[\theta + \sin(\theta)] \quad [0 \leq \theta \leq \pi/2] \tag{1a}$$

and

$$\text{ITD} = (a/c)[\pi - \theta + \sin(\theta)] \quad [\pi/2 \leq \theta \leq \pi], \tag{1b}$$

where θ is the azimuth in radians ($0 \leq \theta \leq \pi$) for the source measured from the forward direction, a is the head radius, and c is the speed of sound. The first of these formulas is for a source in front of the head (where the nose is), and the path to the occluded ear is around the front of the head. The second formula is for a source in back (source azimuth greater than 90°) so that the path to the occluded ear is also in back. For this and other sections of this article, it is assumed that the head is left-right symmetrical having reflection symmetry through the mid-sagittal plane. Therefore the sign of the ITD will always be positive when the source is to the right of the mid-sagittal plane, and it is enough to give formulas for a source on the right with azimuths between 0° and 180°. ITDs for sources on the left are the same except that the signs of θ and the ITD are both reversed.

Because the standard Woodworth model assumes that the ear angle is 90°, this form of the model is front-back symmetrical and exhibits a cone of confusion, as noted by Woodworth and Schlosberg (1954). For any source located on the surface of a cone with rotational symmetry about the interaural axis, the ITD will be the same.

B. Exact diffraction calculation

Our test of the Woodworth model is based on an exact diffraction calculation for a rigid, spherical head. The rigidity assumption says that the component of the wave velocity perpendicular to the surface of the head is zero. It corresponds to an infinite impedance discontinuity at the surface. Such an assumption is valid for a head in air. It is not valid for a head in other media such as water, where the impedance discontinuity is not so large (Hollien and Rothman, 1971; Wells and Ross, 1980), but we will not consider such cases here. Consistent with the assumptions of the Woodworth model, the diffraction calculation assumes a plane-wave incident on a spherical head with an ear angle of 90°.

The diffraction calculation of the pressure on the surface of a rigid sphere is an infinite sum of partial waves,

$$p(\theta') = \left(\frac{p_o}{ka}\right)^2 \sum_{n=0}^{N} \frac{i^{n+1}(2n+1)P_n(\cos\theta')}{h'_n(ka)}, \tag{2}$$

where $p(\theta')$ is the complex pressure at a point on the sphere, and θ' is the angle between a radius to that point and a directed line to the source. Pressure p_o is a reference, equal to what the pressure would be at the location of the center of the head if the head were absent. Function P_n is a Legendre polynomial, and h'_n is the derivative of a spherical Hankel function of the second kind with respect to its argument. The argument ka is the product of the wave number k (defined as 2π divided by the wavelength) and the head radius a, which is nominally 87.5 mm (Hartley and Fry, 1921; Algazi *et al.*, 2001). The upper limit on the sum, N, must be infinite to

obtain an exact solution, but because the sum converges, N is limited in practical computation. Larger values of N are required for greater precision or for higher frequencies, where the sum converges more slowly.

We are interested in the pressure on the sphere where the ears are located, at angle θ_E clockwise and counterclockwise from the forward direction. To be clear, by definition θ_E is the same positive number for both ears. For instance, for antipodal ears $\theta_E = 90°$. Therefore to compute the pressure at the right ear (nearer the source) $\theta' = \theta_E - \theta$, and for the left ear (farther from the source) $\theta' = \theta_E + \theta$. That is how θ' in Eq. (2) is determined from the ear angle θ_E and the source azimuth θ for $\theta > 0$.

The phase of a signal, ϕ, is given by the imaginary part of the natural logarithm of the pressure at the ear. For the right ear, for example, $\phi_R = \text{Im}\{\ln[p(\theta_E - \theta)]\}$. The ITD is the interaural phase difference (in radians) divided by the angular frequency $\omega = 2\pi f$, i.e.,

$$\text{ITD} = \text{Im}\{\ln[p(\theta_E + \theta)/p(\theta_E - \theta)]\}/\omega \tag{3}$$

with θ_E set equal to $\pi/2$.

Equations (2) and (3) lead to an exact solution for the ITD, and that solution ought to be an adequate test for any alternative calculation such as the Woodworth formula. However, several years ago we had occasion to compare the predictions of that solution with interaural phase measurements made on an 87.5-mm sphere in an anechoic room using an array of 13 loudspeakers separated by 7.5°. Measurements for 15 frequencies spanning the range from 0.2 to 6 kHz therefore led to 195 comparisons. Because of geometrical inaccuracies in the array, measurements were made twice, first clockwise (speakers to the right of the sphere), then counterclockwise (speakers to the left of the sphere). The two measurements differed by an average of about 20° of interaural phase angle. In the comparison, the solution from Eqs. (2) and (3) split the difference between the two measurements on 156 of the 195 comparisons, demonstrating good experimental correspondence between model and measurement.

Using Eqs. (2) and (3), we computed the ITD for frequency f equal to 0.5 kHz, a low frequency. The frequency is low enough that the ITD from the full diffraction calculation is approximately given by the low-frequency limit formula, ITD $= (3a/c)\sin(\theta)$ (not shown in figures). The maximum error made by the low-frequency limit occurs near 30° where the approximation is about 16 μs too low. At 90°, the low-frequency limit approximation is 6 μs too high. By contrast, Fig. 1 shows that the frequency-independent Woodworth formula seriously underestimates the ITD for 0.5 kHz. The error can be as large as 180 μs (azimuth of 60°). At 0.5 kHz, the ratio of wavelength to head radius is 7.9. Similar errors can be expected for the head of any animal whenever that ratio is as large as that. Calculations of the dispersion for a spherical head with a radius of 87.5 mm show that 0.5 kHz is the upper edge of the low-frequency region where the low-frequency limit applies. For all lower frequencies, the limit continues to apply, but as the frequency increases to 2 kHz, the ITD for a given azimuth decreases rather rapidly (e.g., Constan
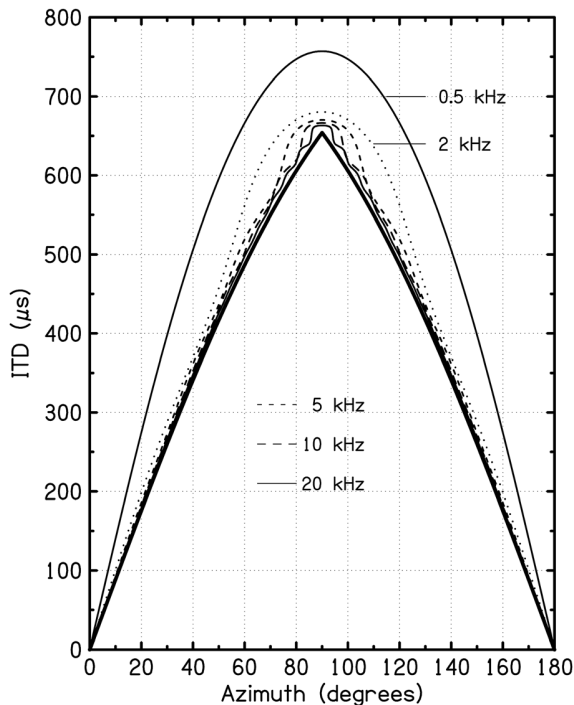
FIG. 1. Interaural time difference as a function of azimuth for plane-wave incidence and antipodal ears. The heavy line is from the Woodworth formula in Eq. (1). Lighter lines come from the exact diffraction formula for frequencies of 0.5, 2, 5, 10, and 20 kHz.
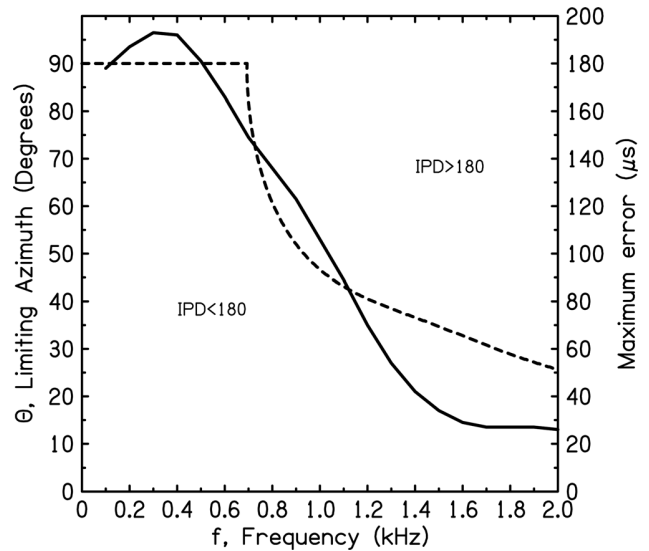

FIG. 2. Limits on ITDs in narrow-band signals caused by the π-limit. The dashed line shows the azimuth and frequency for which the IPD is 180° according to the spherical head model (the π-limit). The solid line (axis labels on the right) indicates the maximum error of the Woodworth formula within the boundaries of azimuth and frequency allowed by the π-limit.

and Hartmann, 2003, Fig. 1). As a result, the Woodworth formula is superior to the low-frequency limit (smaller error) when the frequency is greater than 1.5 kHz.

Using Eqs. (2) and (3), we computed the ITD for 2, 5, 10, and 20 kHz, where the ratio of wavelength to head radius is, respectively, 2.0, 0.79, 0.39, and 0.20. As often noted, the sum over partial waves converges slowly when the frequency is high (large ka), and to obtain acceptable accuracy for ITD, our calculation for 20 kHz required as many as $N = 54$ terms in the sum. Using such a large number of terms in a brute-force calculation is not the standard approach to computing the high-frequency limit of a partial wave sum such as Eq. (2), although it is possible to do with good precision on modern computers. The standard approach is to use the Sommerfeld–Watson transformation (Junger and Feit, 1986). That approach leads to new physical insight. For instance, it shows that the creeping wave decays exponentially with increasing path angle around the head (Pierce, 1981). However, by summing the terms for finite frequencies, we are able to observe the errors made by the Woodworth model when the frequency is not very high, as shown in Fig. 1. For frequencies higher than 0.5 kHz, the largest errors tend to occur for azimuths between 70° and 85°: 86 μs at 2 kHz, 51 μs at 5 kHz, 32 μs at 10 kHz, 17 μs at 20 kHz.

In a context where the signals are narrow band, such as sine tones, there are additional considerations. The highest frequency at which human listeners are sensitive to the ITD in the fine structure of a waveform is about 1.5 kHz (Brughera et al., 2013). For that frequency, the error in the Woodworth formula becomes as large as 100 μs at an azimuth of 63°. Also, the ITD is not useful if the corresponding interaural phase difference (IPD) is more than 180°. The dashed line in Fig. 2 shows the azimuth for which the IPD becomes as large as 180° for a frequency as high as f, shown on the horizontal axis. The solid line shows the maximum error, as a function of frequency, given that the azimuth is less than shown by the dashed line. The limited azimuth has the effect of limiting the maximum error made by the Woodworth formula for practical circumstances. When the frequency is less than 0.9 kHz, the azimuth at which the maximum error occurs is between 50° and 60°. When the frequency is greater than 0.9 kHz, the azimuth of maximum error follows the dashed curve.

III. EXTENDING WOODWORTH'S MODEL

Our extensions of Woodworth's model are expected to be useful in computing ITDs for clicks, high-frequency tones, and high-frequency noise bands, where the assumptions of a ray-tracing model are approximately realized. The extensions involve the same basic wave physics as the original model with the ITD computed from the extra path length to the far ear. The path lengths are again composed of straight-line paths and creeping waves. Again, only the shortest path is included in the calculation for waves that creep to an occluded ear, a step that is made plausible by the fact that creeping wave amplitudes decay exponentially. We will consider situations in which the longest and shortest paths are not dissimilar in Sec. III B 1.

The three conditions involved in extending the model are shown in (a), (b), and (c) of Fig. 3. Condition (a) is the original model with plane-wave incidence and antipodal ears. Condition (b) relaxes the restriction to antipodal ears, permitting arbitrary ear angles, but retains the plane-wave incidence. Condition (c) allows for both arbitrary ear angles and finite source distance. Labels (a), (b), and (c) are then
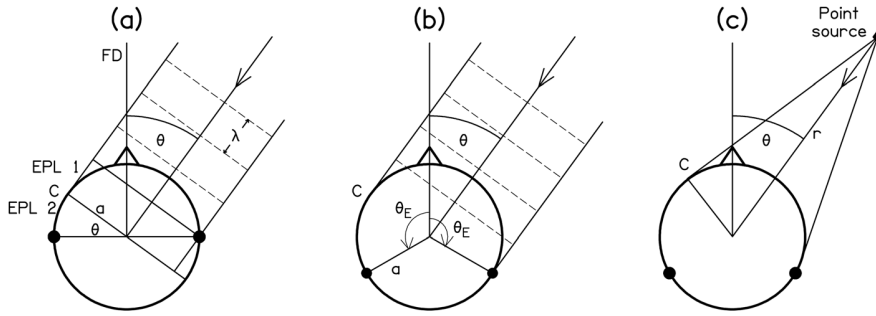
FIG. 3. An illustration of the three geometrical conditions involved in extending the Woodworth model. Condition (a) is the original Woodworth model with infinite source distance (plane wave incidence) and antipodal ears (solid dots) ($\theta_E = 90°$). Condition (b) maintains plane wave incidence but allows for arbitrary ear angles θ_E. Condition (c) allows for a finite source distance as well as arbitrary ear angles.

also used to label the relevant equations and then used again in Fig. 4, which specifies the regions of validity of those equations.

Because the basic physical assumptions are similar, the validity of the extensions continues to be limited to high-frequency sounds where the wavelength is considerably smaller than the head radius.

A. Plane wave source, antipodal ears

The original Woodworth model for an infinite source distance and ear angles of 90° leads to the two formulas for the ITD given in Eqs. (1a) and (1b), repeated here and relabeled to be consistent with Fig. 4,

$$\text{ITD} = (a/c)[\theta + \sin(\theta)] \quad [\theta \leq \theta \leq \pi/2] \tag{a2}$$

and

$$\text{ITD} = (a/c)[\pi - \theta + \sin(\theta)] \quad [\pi/2 \leq \theta \leq \pi], \tag{a3}$$

the regions of validity of these two equations are shown in Fig. 4(a).

B. Arbitrary ear angles

More realistic models of the head allow for ear angles greater than 90°, i.e., $\theta_E > 90$. Hartley and Fry (1921)

measured the ear separation to be 165°, corresponding to an ear angle of $(360 - 165)/2 = 97.5°$ in a spherical-head context. Duda and Martens (1998) used 100°, as did Treeby et al. (2007). Behind-the-ear hearing aids or cochlear implant microphones involve even larger ear angles. When the ears are no longer antipodal, the symmetry between front and back is broken and the surfaces of binaural confusion are no longer circular cones. The back of the (otherwise uniformly spherical) head differs from the front only because the ears are on the back.

The purpose of this section is to show how to extend the Woodworth model to other ear angles θ_E, where $90 \leq \theta_E \leq 180°$ while retaining the incident plane wave assumption. As observed by Duda and Martens (1998), the ingredients for this treatment consist of only two equations, one for an occluded ear and one for an unoccluded ear. However, the practical implementation of those equations requires the user to observe geometrical limiting conditions.

In the end, there are actually five separate formulas required to compute the ITD in general. The correct formula to use is determined by a set of inequalities for azimuth θ and ear angle θ_E. The inequalities are complicated, and they are best expressed in graphical form as shown by the lines in Fig. 4(b). For instance, if θ is below the line $\theta = \theta_E - 90$ and θ is also below the line $\theta = 180 - \theta_E$, then the right equation to use is Eq. (b1). Again, if the ear angle is $\theta_E = 120°$, then we would use Eq. (b1) for azimuths $0 < \theta < 30°$, Eq. (b2) for
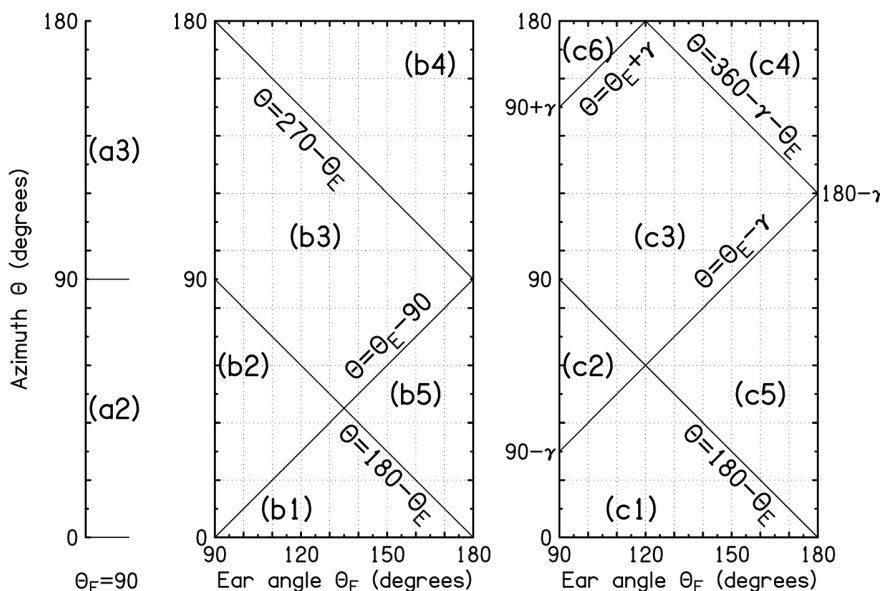
FIG. 4. Regions of azimuth and ear-angle defining the ranges of validity for equations in the extended Woodworth model. (a) Plane-wave incidence and antipodal ears. (b) Plane-wave incidence and general ear angle. (c) Point source and general ear angle. Angle γ is defined by $\cos \gamma = 1/\rho = a/r$. In the limit that $\theta_E = 90°$, (b) becomes equivalent to part (a). In the limit that a/r is zero so that $\gamma = 90°$, (b) and (c) become the same.

$30° < \theta < 60°$, Eq. (b3) for $60° < \theta < 150°$, and Eq. (b4) for $150° < \theta < 180°$.

Geometrical descriptions of the regions are as follows:

(1) Region b1: Both ears are occluded and the path to the far ear is in front.
(2) Region b2: Only the far ear is occluded and the path to the far ear is in front.
(3) Region b3: Only the far ear is occluded and the path to the far ear is in back.
(4) Region b4: Neither ear is occluded (the source must be in back).
(5) Region b5: Both ears are occluded and the path to the far ear extends from front to back.

The equations are as follows:

$$\text{ITD} = (2a/c)[\theta], \tag{b1}$$

$$\text{ITD} = (a/c)\left[-\pi/2 + \theta + \theta_E + \cos(\theta - \theta_E)\right], \tag{b2}$$

$$\text{ITD} = (a/c)\left[3\pi/2 - \theta - \theta_E + \cos(\theta - \theta_E)\right], \tag{b3}$$

$$\text{ITD} = (a/c)[\cos(\theta - \theta_E) - \cos(\theta + \theta_E)], \tag{b4}$$

$$\text{ITD} = (2a/c)[\pi - \theta_E]. \tag{b5}$$

The results from the formulas, as determined by the appropriate regions in Fig. 4(b), are illustrated in Fig. 5, which shows the dependence of ITD on azimuth for five different ear angles, 90°, 110°, 130°, 150°, and 170°. To be sure, an anatomy with the ears only 20° apart at the back of the head (ear angle of 170°) is fanciful, but it is included for mathematical completeness.

In the special case that ear angle θ_E is 90°, Fig. 4(b) shows that the equations progress directly up the left edge from region b2 to region b3, as expected from Fig. 4(a). Then the plot of ITD as a function of azimuth in Fig. 5 is the familiar simple case (incident plane waves and antipodal ears). The peak of the ITD function is at a maximum for this ear angle of 90°, here 654 μs. For a general ear angle, the peak of the ITD occurs at an azimuth of $\theta = 180 - \theta_E$, where the source direction is exactly opposite to the far ear angle. At this point, the ITD function has a discontinuous derivative, indicating that something has gone wrong.

1. Correcting the Woodworth model

What is wrong with the Woodworth model is that it considers only the path around one side of the head. Because of the exponential decay of creeping waves, it may be a reasonable assumption to ignore the longer path when the path lengths are quite different. But when the far ear is nearly opposite to the source direction, the path in front of the head and the path in back are about the same length. Then waves along both paths contribute about equally. The thin solid line in Fig. 1 for 20 kHz actually shows the interference between the two waves. The interference can be understood quantitatively: The oscillations away from the peak at 90° have an expected periodicity of one wavelength, or 17 mm. For a deviation δ (in radians) away from 90°, the path length difference is $2a\delta$. The thin solid line appears to have a periodicity of about 6°, corresponding to a path length difference of 18 mm, close to the expected value of 17 mm.

When both paths contribute about equally, it is wrong to include only one path. A more logical treatment adds the creeping waves around both sides of the head. It is not hard to add the two creeping waves for the simplest case—incident plane wave and antipodal ears—if the two path lengths are so similar that the two waves can be assumed to have the same amplitude. The solution for θ near 90° is no longer $\text{ITD} = (a/c)(\theta + \sin\theta)$. Instead the explicit linear dependence on θ is cancelled, and the ITD becomes $\text{ITD} = (a/c)(\pi/2 + \sin\theta)$, a result with a continuous derivative at $\theta = \pi/2$.

One can go further using the fact that the creeping wave amplitudes decay exponentially with distance around the circumference as $\exp(-\theta/d)$, where d is a constant of attenuation. Then the solution to the sum of two creeping waves leads to an ITD that depends on frequency, thereby losing the important simplicity of the Woodworth model. However, an expansion to lowest order in $\theta - \pi/2$ is again frequency independent. In the limit that the incident angle approaches 90°, $\text{ITD} = (a/c)[1 + \pi/2 - (2 + d)(\theta - \pi/2)^2/(2d)]$. Therefore the top of the function is parabolic and no longer pointed.

C. Finite source distance

An alternative to the incident plane-wave is a point source at a distance r from the center of the head as shown in Fig. 3(c). The effects of finite source distance can be expressed in terms of parameter $\rho = r/a$, which is the source distance in units of the head radius ($\rho \geq 1$), and parameter $\gamma = \cos^{-1}(a/r)$ ($0 \leq \gamma \leq \pi/2$). Figure 4(c) has labels for general values of ρ and γ, but the actual drawing corresponds to the special case where $\rho = 2$ so that $\gamma = 60°$. As shown in Fig. 4(c), the finite distance causes a sixth region to drop down from above $\theta = 180°$, with the following geometrical description:
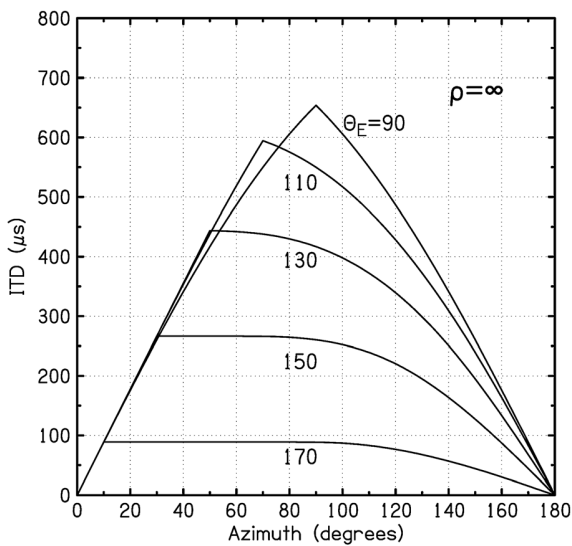

FIG. 5. ITD from the extended Woodworth formula as a function of plane-wave source azimuth for five ear angles as shown. Parameters were $a = 87.5$ mm, $c = 344\,000$ mm/s.

J. Acoust. Soc. Am., Vol. 135, No. 2, February 2014

N. L. Aaronson and W. M. Hartmann: Woodworth model 821

(1) Region c6: Both ears are occluded and the path to the far ear begins with a source in back. The geometrical descriptions of the other regions in Fig. 4(c) are the same as for the corresponding regions in Fig. 4(b). There are two intersections of interest in Fig. 4(c). The lower intersection (at $\theta = 60°$) occurs for $\theta_E = (180 + \gamma)/2$. The higher intersection (at $\theta = 180°$) occurs for $\theta_E = 180 - \gamma$. In general, these intersections occur at different values of θ_E, but for the special case shown, where $\gamma = 60°$, they happen to be the same.

The equations for ITDs are as follows:

$$ITD = (2a/c)[\theta], \tag{c1}$$

$$ITD = (a/c)[\theta + \theta_E - \gamma + \sqrt{\rho^2 - 1} \\ - \sqrt{1 + \rho^2 - 2\rho\cos(\theta - \theta_E)}], \tag{c2}$$

$$ITD = (a/c)[2\pi - \gamma - \theta - \theta_E + \sqrt{\rho^2 - 1} \\ - \sqrt{1 + \rho^2 - 2\rho\cos(\theta - \theta_E)}], \tag{c3}$$

$$ITD = (a/c)[\sqrt{1 + \rho^2 - 2\rho\cos(\theta + \theta_E)} \\ - \sqrt{1 + \rho^2 - 2\rho\cos(\theta - \theta_E)}], \tag{c4}$$

$$ITD = (2a/c)[\pi - \theta_E], \tag{c5}$$

$$ITD = (2a/c)[\pi - \theta_E]. \tag{c6}$$

Although the equations for regions c5 and c6 are the same, they apply to distinct geometrical situations and disconnected regions in Fig. 4. Region c1, with no distance dependence, was identified by Woodworth (1938) as the correct solution for a source close to the head but without qualification or definition of "close." Region c3 was identified by Molino (1973).[2]

D. Illustrations

The formulas, as determined by the appropriate regions, are illustrated in Figs. 6 and 7 which, like Fig. 5, show the dependence of ITD on azimuth for five different ear angles, 90°, 110°, 130°, 150°, and 170°.

The condition $\rho = 1$ in Fig. 6, where the source is on the surface of the head, leads to particular insight. In this case, angle γ becomes zero. Then region c4 disappears off the top of Fig. 4 and regions c2 and c3 shrink to zero size. Then as θ increases from 0° to 180°, the applicable regions are c1, c5, and c6. For ear angles near 90°, regions c1 and c5 dominate, which is why Woodworth recommended Eq. (c1) for sources close to the head. The flat regions in Fig. 6 (region c5) begin and end at $180 - \theta_E$ and θ_E.

The condition $\rho = 2$, where the source distance is twice the head radius, corresponds to the particular conditions used in Fig. 4(c). The ITD is shown in Fig. 7, where it is evident that the ITD function is a mixture of Fig. 6 ($\rho = 1$), with long flat regions in the middle, and Fig. 5 ($\rho = \infty$), with smaller peaks and slowly dropping ITD as θ approaches 180°. Figure 7 shows that as a crude guide to intermediate values of ρ, one can begin with the extreme values for ρ in Figs. 5 and 6 and interpolate by eye.
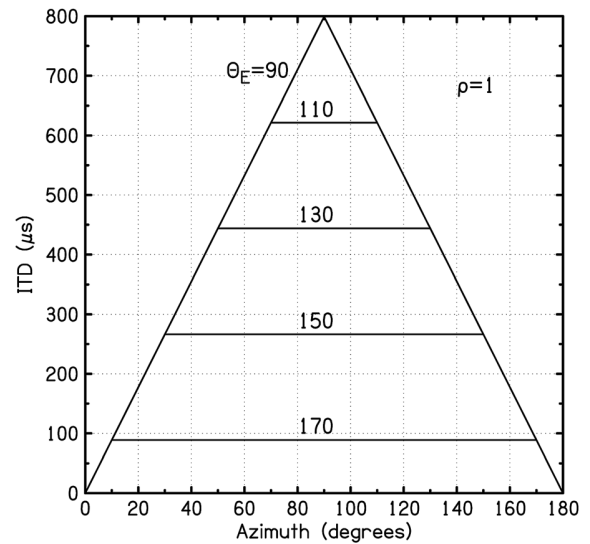

FIG. 6. ITD from the extended Woodworth formula for five ear angles as shown for a source on the surface of the head, $\rho = 1$.

As a check on the calculations, we considered the condition $\rho = 1000$, where the source is so far from the head that the plane-wave approximation applies well. The calculation from the formulas of Sec. III C agree with those from Sec. III B, and Figs. 4(b) and 5 apply.

IV. SUMMARY

The Woodworth model and formula for the ITD around a spherical head were compared with the exact solution for the ITD from the diffraction formula. It was concluded that for tonal or narrow-band sources, the low-frequency limit of the diffraction formula is a better estimate of the ITD than the Woodworth formula for frequencies below 0.8 kHz. The Woodworth formula provides a better estimate for frequencies above 1.5 kHz. Between 0.8 and 1.5 kHz, the relative error depends on azimuth.
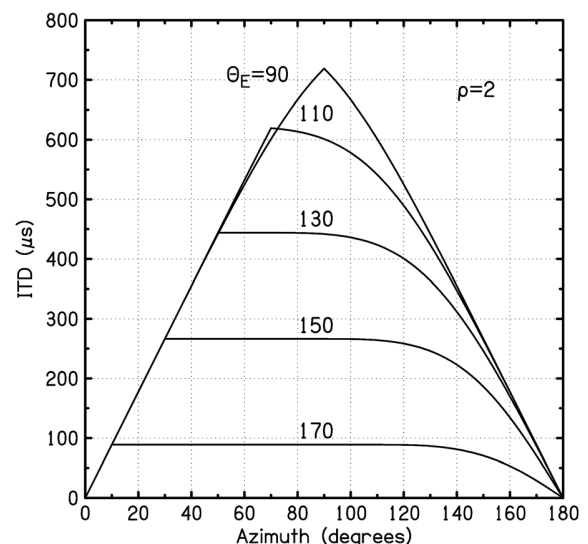

FIG. 7. ITD from the extended Woodworth formula for five ear angles as shown for a source of sound located at twice the head radius, $\rho = 2$.

The characteristic kink produced by the Woodworth formula was shown to be an artifact without realistic physical foundation. As a frequency-independent equation, the Woodworth formula is valuable for broadband noise or clicks or tones with high frequency. Using the Woodworth model in those cases was made more practical by extending it so that it applies to all possible ear angles and to all possible source distances.

The geometry in this article has mainly been confined to sources in the azimuthal plane because of the emphasis on general ear angle. By contrast, if the ear angle is limited to $90°$, sources with an elevation out of the azimuthal plane are easily tractable through cones of confusion. The ITDs are the same for all sources located on the surface of a cone of confusion, independent of source distance. The cones of confusion are uniquely defined by a single angle, the lateral angle (Morimoto and Aokata, 1984; Macpherson and Middlebrooks, 2002), which is a function of both azimuth and elevation. However, when the ear angle differs from $90°$, the surfaces of constant ITD become complicated objects. The description of these objects is beyond the scope of this article and would be an interesting topic for future mathematical research.

ACKNOWLEDGMENTS

[1]The formula has sometimes been called the "Woodworth-Schlosberg formula" because it appeared in the 1954 and 1962 textbooks by those authors (Woodworth and Schlosberg, 1954, 1962), e.g., Duda and Martens (1998). In this article, we follow Green (1976) in calling it the "Woodworth formula" because the formula appears in the 1938 textbook by Woodworth alone.

[2]Apparently Molino (1973) interpreted the angle between the ears reported by Hartley and Fry (1921) to mean that the angle around the front of the head is smaller than the angle around the back. Therefore when Molino derived an equation for a source in front of the listener, he produced Eq. (c3). However, Molino's interpretation was incorrect, and as can be seen in Fig. 4(c), region c3 actually corresponds to a source in back.

Algazi, V. R., Avendano, C., and Duda, R. O. (**2001**). "Estimation of a spherical head model from anthropometry," J. Audio Eng. Soc. **49**, 472–497.

Brown, C. P., and Duda, R. O. (**1998**). "A structural model for binaural sound synthesis," IEEE Trans. Speech Audio Process. **6**, 476–488.

Brughera, A., Dunai, L., and Hartmann, W. M. (**2013**). "Human interaural time difference thresholds for sine tones. The high-frequency limit," J. Acoust. Soc. Am. **133**, 2839–2855.

Carlile, S. (**1996**). "The physical and psychophysical basis of sound localization," in *Virtual Auditory Space: Generation and Applications*, edited by S. Carlile (R.G. Landes Co., Austin, TX), pp. 27–78.

Constan, Z. A., and Hartmann, W. M. (**2003**). "On the detection of dispersion in the head-related transfer function," J. Acoust. Soc. Am. **114**, 998–1008.

Duda, R. O., and Martens, W. L. (**1998**). "Range dependence of the response of a spherical head model," J. Acoust. Soc. Am. **104**, 3048–3058.

Feddersen, W. E., Sandel, T. T., Teas, D. C., and Jeffress, L. A. (**1957**). "Localization of high frequency tones," J. Acoust. Soc. Am. **29**, 988–991.

Green, D. M. (**1976**). *An Introduction to Hearing* (Erlbaum, Hillsdale, NJ), pp. 202–203.

Hartley, R. V. L., and Fry, T. C. (**1921**). "The binaural localization of pure tones," Phys. Rev. **18**, 431–442.

Hollien, H., and Rothman, H. (**1971**). "Underwater speech communication" (United States Office of Naval Research, University of Florida, Communication Sciences Laboratory).

Junger, M. C. and Feit, D. (**1986**). *Sound, Structures and Their Interaction*, 2nd ed. (MIT Press, Cambridge, MA) [reprinted by the Acoustical Society of America, 1993, pp. 388–396].

Kuhn, G. F. (**1977**). "Model for the interaural time differences in the azimuthal plane," J. Acoust. Soc. Am. **62**, 157–167.

Macpherson, E. A., and Middlebrooks, J. C. (**2002**). "Listener weighting of cues for lateral angle: The duplex theory of sound localization revisited," J. Acoust. Soc. Am. **111**, 2219–2236.

Molino, J. (**1973**). "Perceiving the range of a sound source when the direction is known," J. Acoust. Soc. Am. **53**, 1301–1304.

Morimoto, M., and Aokata, H. (**1984**). "Localization cues of sound sources, in the upper hemisphere," J. Acoust. Soc. Jpn. **5**, 165–173.

Nam, J., Abel, J. S., and Smith, J. O. (**2008**). "A method for estimating interaural time difference for binaural synthesis," in *125th Audio Engineering Society Convention*, San Francisco, p. 125.

Pierce, A. D. (**1981**). *Acoustics: An Introduction to its Physical Principles and Applications* (McGraw-Hill, New York), p. 475.

Rayleigh, J. W. S. (**1896**). *The Theory of Sound, Vol. II* (Macmillan, London), p. 272.

Rschevkin, S. N. (**1963**). *A Course of Lectures on The Theory of Sound*, translation by P. E. Doak (Pergamon, McMillan, New York), pp. 350–370.

Schnupp, J. W. H., Booth, J., and King, A. J. (**2003**). "Modeling individual differences in ferret external ear transfer functions," J. Acoust. Soc. Am. **113**, 2021–2030.

Treeby, B. E., Paurobally, R. M., and Pan, J. (**2007**). "The effect of impedance on interaural azimuth cues derived from a spherical head model," J. Acoust. Soc. Am. **121**, 2217–2226.

Wells, M. J., and Ross, H. E. (**1980**). "Distortion and adaptation in underwater sound localization," Aviat. Space Environ. Med. **51**(8), 767–774.

Woodworth, R. S. (**1938**). *Experimental Psychology* (Holt, New York), pp. 520–523.

Woodworth, R. S., and Schlosberg, H. (**1954**). *Experimental Psychology* (Holt, Rinehard, and Winston, New York), pp. 349–361.

Woodworth, R. S., and Schlosberg, H. (**1962**). *Experimental Psychology* (Holt, New York), pp. 348–361.